RESEARCH ARTICLE

WILEY

A wide-line low frequency electron paramagnetic resonance spectrometer

Lauren E. Switala | William J. Ryan | Merlin Hoffman | Stephany Javier | Baron E. Black | Joseph P. Hornak

Magnetic Resonance Laboratory, Rochester Institute of Technology, Rochester, NY, USA

Correspondence

J. P. Hornak, Magnetic Resonance Laboratory, Rochester Institute of Technology, Rochester, NY, USA. Email: jphsch@rit.edu

Funding information

NSF Physics Directorate REU program "Imaging in the Physical Sciences", Grant/ Award Number: 1359361

Abstract

A continuous wave, homodyne, low frequency electron paramagnetic resonance spectrometer is described which can accommodate 15 cm diameter objects. The spectrometer can utilize small volume and surface coil probes operating between 100 and 500 MHz. The magnetic field can be scanned between 0 and 35 mT and is thus suitable for g < 2 spins and wide absorption lines. The spectrometer can record conventional field swept, field cycled, and spatially resolved spectra. Details of the instrument design and representative spectra from six different samples are presented. This design has applications to study objects with cultural heritage significance.

KEYWORDS

electron paramagnetic resonance, electron paramagnetic resonance instrumentation, LFEPR, low frequency electron paramagnetic resonance spectroscopy, surface coils

1 | INTRODUCTION

Electron paramagnetic resonance (EPR) and electron magnetic resonance (EMR) spectroscopy are used to study paramagnetic and ferromagnetic materials. The spectrometers can probe the real (χ') and imaginary (χ'') parts of the magnetic resonance susceptibility (χ) through dispersion and absorption signals. These signals are typically measured by subjecting the sample to an oscillating magnetic field of amplitude B_1 and Larmor frequency v while scanning an applied DC magnetic field (B_0) to observe the resonance condition. Resonance occurs when

$$hv = g\beta B_o \tag{1}$$

where h is Planck's constant, β the Bohr magneton, and g the electron g factor for the sample. The g factor is unique for a sample and provides insight into the environment of the unpaired electron(s). The g factor for a paramagnetic sample can vary from 0.8 to 18,^{2,3} but is most often closer to the Landé g factor of two for the free electron.

Electron paramagnetic resonance spectroscopy is a useful tool for studying objects with cultural heritage importance.4-18 Many pigments used in paintings are paramagnetic. Many clays contain paramagnetic metals, some of which become ferromagnetic upon firing. Marble contains paramagnetic manganese impurities. The aging of resins and varnishes produces free radicals. All these materials possess an EPR signal. EPR is most often performed at v = 9 GHz. Unfortunately, sample size is constrained to mm³-sized objects due to the magnet producing the B_0 field and sample cavity resonator producing the B_1 field, making EPR destructive and invasive for larger objects. Low frequency EPR (LFEPR) overcomes this drawback by operating at a lower frequency where larger volume B_0 magnets and B_1 producing surface coil resonators or probes are more practical. Therefore an LFEPR spectrometer can accommodate large, intact objects making it a nondestructive spectroscopy and opening up new applications for EPR in studying objects with cultural heritage significance.

We previously described a modular, continuous wave (CW) LFEPR spectrometer operating at 200 MHz for 6 cm³ volume, g = 2, narrow line samples with 1.5 mT nuclear hyperfine coupling.¹⁹ This paper describes an enhanced version of this homodyne LFEPR spectrometer with an expanded operating frequency range of 100 < v < 500 MHz, that accommodates 15 cm diameter, liter sized objects, and can scan the magnetic field over a larger range from 0 to 35 mT. The LFEPR spectrometer is thus suitable for wide-line samples with g < 2 spins.

2 | THE LFEPR SPECTROMETER

Electron paramagnetic resonance and EMR spectrometers differ primarily in the material being examined. Both employ a fixed ν and swept B_0 field. B_1 is applied perpendicular to B_0 by a resonator or probe which also detects the signal (S) from the sample. Because the EPR signal is small compared to the noise (N), B_0 magnetic field modulation and phase sensitive detection at frequency f_{Mod} is employed. It is useful to think of the detection scheme in terms of the frequencies present in the spectrometer. The spectrometer excites the sample at frequency v and when scanning B_o through resonance causes an additional lowfrequency signal (f_S) . When magnetic field modulation is employed, the signal coming from the sample at resonance has a frequency $(v + f_{Mod} + f_{S})$. In homodyne detection, this frequency is detected with reference to v in a mixer to produce the sum and the difference of frequencies $(v + f_{Mod} + f_{S})$ and v. The high-frequency component with value equal to the sum of the frequencies $(2v + f_{Mod} + f_{S})$ is filtered out and the low-frequency component at $(f_{\text{Mod}} + f_{\text{S}})$ is retained. Frequency $(f_{\text{Mod}} + f_{\text{S}})$ is sent to a lock-in amplifier for phase sensitive detection at f_{Mod} yielding $f_{\rm S}$. This detection scheme presents spectra which are the first derivative of absorption or dispersion signals. Readers needing more details on CW EPR are directed to one of the more comprehensive texts on EPR. 1,20,21

The description of the LFEPR spectrometer is divided into radio frequency (RF) bridge, magnet, modulation, probes, and control subsystem components. Figure 1 presents a block diagram of these spectrometer subsystems. The choice of specific components used in the spectrometer are not necessarily optimal, but is based on availability and compatibility with other components already in use in the spectrometer.

2.1 | RF bridge

The RF bridge employs a homodyne detection system depicted in Figure 1. All components of the bridge are specified to operate between 100 and 500 MHz and are interconnected with 50 Ω coaxial cable with BNC connectors. The frequency source (RF1) is a 500 MHz frequency synthesizer

(PTS-500; Programmed Test Sources, Littleton, MA, USA). The output from the synthesizer is divided into two equal parts for the sample and reference arms of the bridge by power divider PD1. The sample arm power can be attenuated by up to 70 dB in 10 dB steps using a rotary attenuator (A1) before it is sent to the sample probe via a hybrid tee (T1). A circulator can be substituted for the hybrid tee and will give 3 dB more power but a narrower ~20 MHz operating frequency range. The hybrid tee is connected to the probe via a 122 cm length of cable. The output of the hybrid tee is connected to the R port of a doubly balanced mixer (DBM) detector D1.

The L port of the DBM is derived from the reference arm. The reference arm contains an attenuator (A3) to bias the DBM for maximum signal and a phase shifter (P1) to match the phase of the sample and reference arms. In our spectrometer, the phase shifter is a length of cable. The length of phase cable (L_{ϕ}) needed to bring the reference arm RF in phase with the sample arm RF at frequency ν can be calculated from

$$L_{\phi} = (L_{\rm S} - L_{\rm R}) \pm n(kc/\nu) \tag{2}$$

where $L_{\rm S}$ and $L_{\rm R}$ are, respectively, the sample and reference arm lengths, k the propagation factor for RF in the cable, c the speed of light, and n is an integer. The optimal situation is when n = 0 implying $L_{\rm S} = L_{\rm R} + L_{\rm \phi}$. Solutions to Equation 2 become more cumbersome as small differences in ν can require different $L_{\rm \phi}$ cables.

When the RF from the sample and reference arms are in phase, the DBM provides the absorption signal, and when they differ by $\pi/2$ radians, the dispersion signal. The low pass filter (F1) on the output removes the $(2v + f_{\text{Mod}} + f_{\text{S}})$ frequency and sends $(f_{\text{Mod}} + f_{\text{S}})$ to the lock-in amplifier.

To either side of the hybrid tee are two double throw single pole switches (SW1,2) which either connect the tee or probe to attenuator A1 and detector D1, or to an RF sweeper (RF2) used for tuning the probe. In the tune mode, the swept frequency output of a frequency sweeper (Wavetek 7062, JDS Uniphase, Milpitas, CA, USA) is connected to the input port of the hybrid tee and the output to a diode detector in the sweeper. The scope out of the sweeper is connected to the X and Y channels of an oscilloscope to display reflected power from the probe as a function of frequency. Since the reference port of the hybrid tee is terminated to a 50 Ω terminator, a zero output on the oscilloscope represents a condition where the probe is tuned to 50 Ω and no power is reflected from the probe. From the reference arm, -10 dB of the power is used as a frequency marker in the sweeper to allow the synthesizer frequency to be set to the resonance frequency of the probe. This frequency is also used for a frequency counter (FC1; HP5385a; Agilent, Santa Clara, CA, USA).

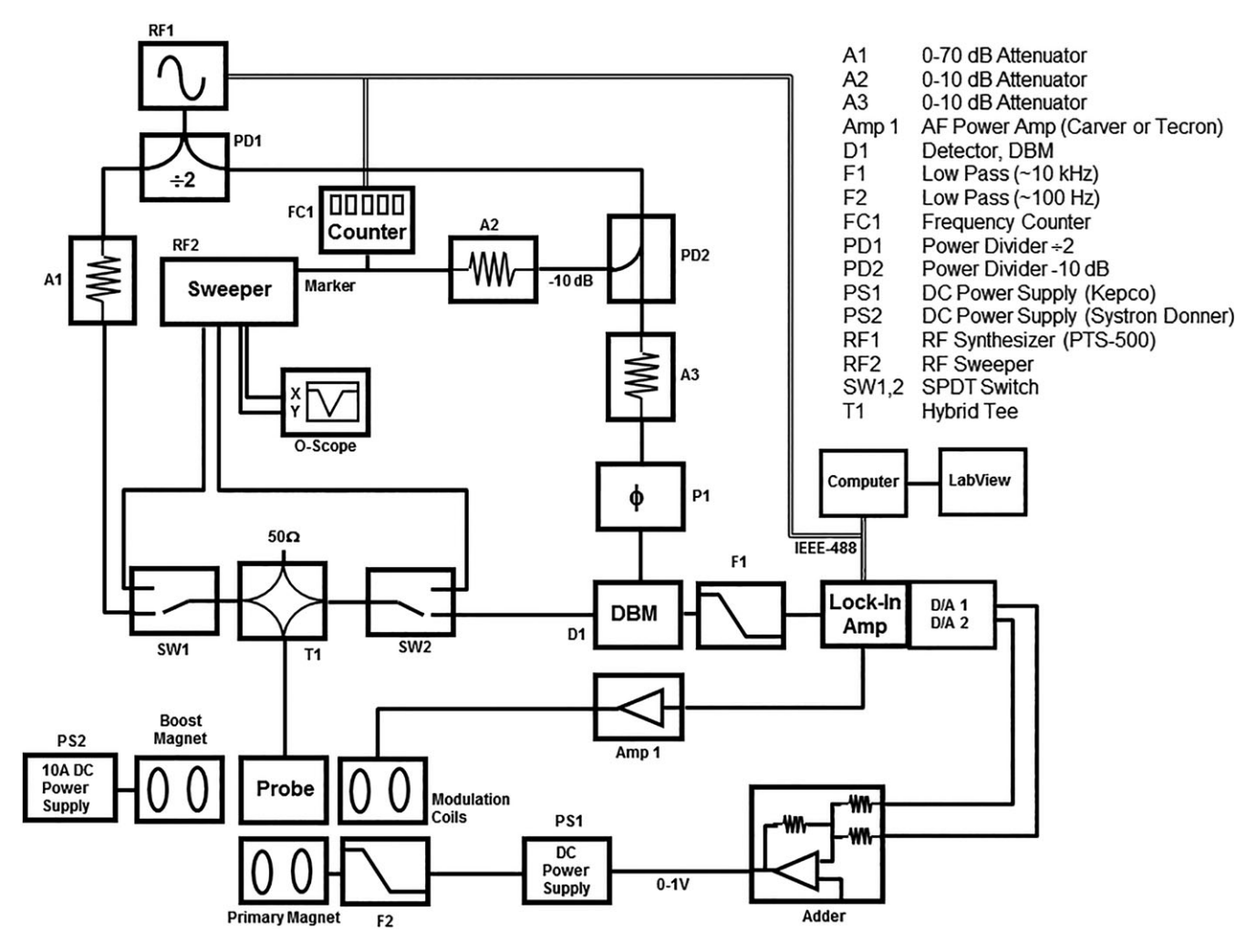


FIGURE 1 Block diagram of the 100-500 MHz low frequency electron paramagnetic resonance spectrometer depicting the radio frequency bridge, magnet, field modulation, probe, tuning, and control subsystems

2.2 | Field modulation system

The magnetic field modulation system consists of an audio frequency source, amplifier, and modulation coil. The source is a lock-in amplifier (SRS-830; Stanford Research Systems, Sunnyvale, CA, USA), capable of delivering a 0-50 kHz frequency, 0-1 V_{PP} amplitude, sine wave. This sine wave is sent to an audio frequency, power amplifier (Caver TFM-15, Jade Design, Franklin, TN, USA or Techron 7570, AE Techron, Elkhart, IN, USA). The Caver TFM-15 is used to drive a 4.3-cm saddle style, 13 Ω , modulation coil on the single turn solenoid (STS). The Techron 7570 is used with the surface coils and drove a larger volume Helmholtz pair or solenoid modulation coils. The Helmholtz pair has a 15 cm inside diameter (ID) and is wound with 200 turns of #10 round, copper wire for a 1.8 Ω total impedance. The solenoidal coil has a 10 cm ID and 8.6 cm length, and is wound with 155 turns of square #14 copper wire yielding a 2.3 Ω impedance.

Two factors influence the choice of the modulation frequency: the phase noise from the RF source and the skin depth at the modulation frequency of any materials between the modulation coils and the sample. In general, the phase noise of an RF source decreases with frequency offset from v. If the signal from the sample has frequency $(v + f_{\text{Mod}} + f_{\text{S}})$, the largest possible f_{Mod} should be chosen to minimize the phase noise. The attenuation of the field modulation increases as f_{Mod} increases due to the effects of skin depth. The choice of f_{Mod} is always the result of a compromise between attaining the lowest phase noise and the highest field modulation amplitude.

The phase noise of our RF synthesizer relative to the carrier at v(dBc) is -90 at 10 Hz, -120 at 10 kHz, and -125 at 100 kHz. The skin depth in the brass shield of the STS at the same frequencies is 40, 1.27, and 0.4 mm, respectively. We choose a modulation frequency range of 10-20 kHz. The other modulation coils used with the surface coil probes could utilize 50 kHz, the maximum frequency value of the lock-in amplifier.

2.3 | Magnet system

The magnet system consists of a solenoidal electromagnet, a boost magnet, and two DC power supplies. The 30 cm ID, 45 cm length solenoidal electromagnet was described previously. 19,22 This electromagnet is driven with a 0-36 V, 0-30 A DC power supply (Kepco, ATE 36-30 M) whose current is controlled by an external 0-1 V signal. This combination of electromagnet and power supply can produce a 0-18.7 mT magnetic field. For larger magnetic fields, a boost magnet is added inside the solenoidal electromagnet. The boost magnet is the same Helmholtz modulation coil described in the modulation system section. This boost magnet is driven with a 10 A power supply (#3002-1 DC; Systron Donner, Concord, CA, USA) to change the sweep start by ± 16 mT, thus giving a -16 to ± 35 mT sweep range for the spectrometer. Using the Helmholtz modulation coil as the boost magnet limits the modulation coil options to that on the STS probe or the 10 cm diameter solenoidal modulation coil. When the Helmholtz coil is used as a modulation coil, the largest diameter sample accommodated by the spectrometer is 15 cm.

Operating large diameter modulation coils inside the magnet can induce voltages in the magnet windings which interfere with the operation of the magnet power supply. A 400 μF film capacitor is placed across the windings of the electromagnet to serve as a low pass filter when combined with the 3.8 Ω resistance of the magnet.

2.4 | Probes

The probe, with an inductance (L) and capacitance (C), is designed to resonate at

$$v = \frac{1}{2\pi\sqrt{LC}},\tag{3}$$

generate the B_1 field perpendicular to B_0 in the sample, and detect the signal (S) from the sample. The probe is matched to $50~\Omega$ impedance of the RF bridge. Any style probe which resonates between 100 and 500 MHz can be used on the spectrometer. We have utilized three general designs: a STS, a five-turn solenoid, and a seven-turn spiral. The STS is a volume probe meaning that the LC circuit surrounds the sample. The five-turn solenoid and the seven-turn spiral coils are surface coils. They are placed adjacent to the sample and the B_1 RF magnetic field enters perpendicular to the surface of the sample.

The STS resonator is similar in design to that described on the original spectrometer¹⁹ with a few modifications. The diameter of the copper foil cylindrical inductor was decreased to 2 cm while keeping the 15.8 mm sample diameter, thus increasing the filling factor¹ of the resonator. Additionally, four equally spaced, 1 mm wide, circumferential slits were added parallel to the bases of the cylinder. These allow more of the modulation field to penetrate through the STS and into the sample. Seven different STS inserts were constructed on PVC supports, resonating at 150, 205, 251, 299, 354, 400, and 440 MHz. These supports fit inside the previously described shield, coupling loop, and modulation coils.

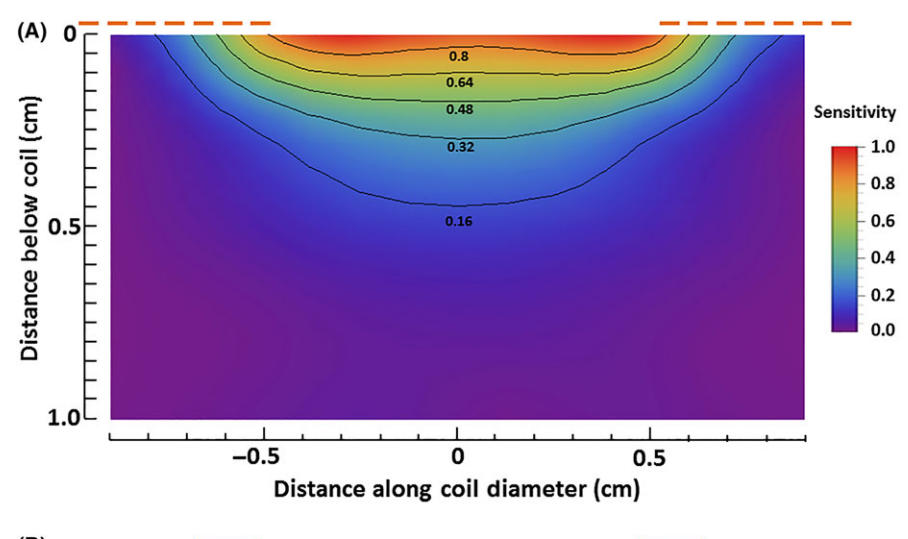
The five-turn solenoid was wound around a 2.9 mm outside diameter, cylindrical polyethylene form with #26 copper wire. A 5 pF, non-magnetic, chip capacitor (American Technical Ceramics Corp [ATC], Huntington Station, NY, USA) brought the LC circuit to resonance at 247 MHz. The LC circuit was inductively coupled to 50 Ω via a two-turn, #30 copper wire coupling loop located coaxially above and opposite the sample end of the solenoid. The impedance was adjusted via a nylon screw which changed the distance between the coupling loop and solenoid.

The second surface coil was a seven-turn, Archimedean, microstrip spiral etched on a single-sided 0.1143 mm thick PTFE 0.0381 mm thick copper circuit board. The equation of the spiral in polar coordinates (r,θ) is

$$r = a + (1/2)b + c\theta \tag{4}$$

where the inner spiral radius a=4.65 mm, the microstrip width b=0.5 mm, c=0.115 mm, and $0 \le \theta \le 14\pi$ radians. The spiral had three gaps along its length at 100, 500, and 645π radians and the last two were spanned by 1 pF ATC chip capacitors. The resultant resonant frequency was 271 MHz. The LC circuit was inductively coupled to 50 Ω via a one-turn, 1.5 cm diameter, #18 copper wire coupling loop located coaxially above and opposite the sample side of the spiral. The impedance was adjusted via a nylon screw which changed the distance between the coupling loop and spiral.

The spatial sensitivity of an STS coil was presented previously.²³ The spatial sensitivity of the surface coils were determined by measuring the peak-to-peak signal (Spp.) from a 1.55 mm diameter, 0.25 mm thick piece of 2,2diphenyl-1-picrylhydrazyl (DPPH; Sigma-Aldrich, Louis, MO, USA) in epoxy at a matrix of locations adjacent to the surface coils. The DPPH sample disc was located on the end of the thin tip of a 15-cm Pasteur pipette and was positioned adjacent to the probe using a twoaxis micrometer positioning system. The sensitivity was calculated from the peak-to-peak EPR signal (SPP). Values of sensitivity for the two coils were normalized and displayed in Figure 2. The location of the surface coil inductor is depicted at the top of each sensitivity plot. The majority of the signal from the spiral surface coil comes from a 1 cm diameter, 4 mm thick disc, while for the five-



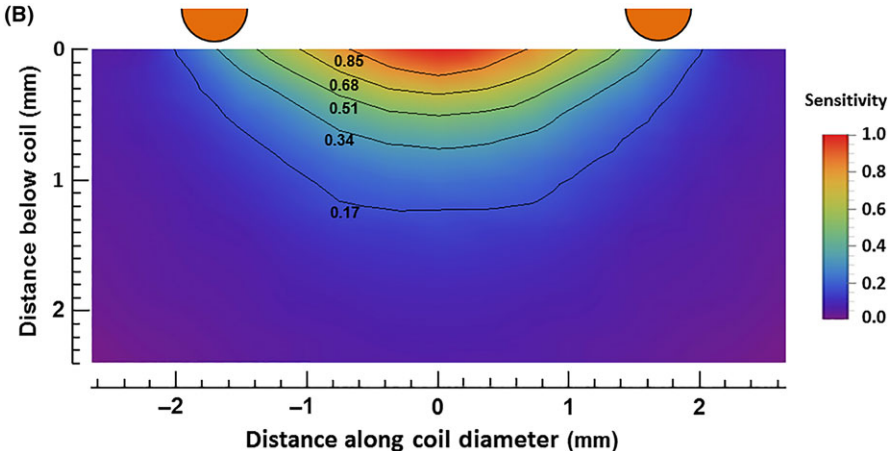


FIGURE 2 Relative sensitivity plots for a plane perpendicular to the surface of the (A) spiral, and (B) solenoidal surface coil probes. The markings above the plots indicate the position of the adjacent inductor of the coil. The sensitivity is normalized to the greatest value in the center of each coil.

TABLE 1 Properties of the different surface coil probes

Туре	Size	v (MHz)	Q	Relative sensitivity
Single turn solenoid	$V = 6.3 \text{ cm}^3$	150	127	0.01
		205	196	0.02
		251	212	0.02
		299	186	0.03
		354	180	0.01
		400	444	0.03
		440	445	0.02
SC	d = 2.9 mm	245	75	1.00
	d = 2 cm	271	109	0.09

turn solenoid the disc has a 2.2 mm diameter and 0.5 mm height.

A comparison of the sizes, resonant frequencies, Q values, and relative sensitivities of the various probes can be found in Table 1. The relative sensitivity values for the nine probe configurations were calculated from the same 1.55 mm disc of DPPH in each coil and normalized to that of the five-turn solenoid. These are

volume limited sample measurements and the filling factor only approached optimal conditions with the fiveturn solenoid coil.

2.5 | Control

The LFEPR spectrometer is controlled by LabView (National Instruments, Austin, TX, USA) code through an IEEE-488 instrument bus. The frequency of the synthesizer is set either manually via the front panel knobs or remotely through the IEEE-488 bus. The lock-in amplifier can also be set remotely or locally over the bus, but data acquisition is only accomplished remotely. The LabView code also sets a voltage on two of the lock-in's digital-to-analog (D/ A) converters for use in controlling the magnetic field. The two voltages, controllable in 1 mV steps between 0 and 10.5 V, are sent to a voltage divider/adder operational amplifier to give the 0-1 V magnet power supply control voltage (V_C) in minimally 0.1 mV steps. The magnetic field is set in the LabView interface as a percent of the maximum possible field ($B_{\rm oMax}$). The $V_{\rm C}$ step size ($\delta V_{\rm C}$) for a B_0 field sweep determines the number of points in a field sweep and is set by the user for each scan. The maximum points in a 100% $B_{\rm oMax}$ spectrum is therefore 10 000. The user also has control over the time the program waits ($t_{\rm Wait}$) at each field value before acquiring the signal and advancing to the next field value. The $t_{\rm Wait}$ value is relevant when choosing the lock-in time constant.

Three LabView programs were written to control the LFEPR spectrometer. All programs give the operator control over the number of points acquired and t_{Wait} at each point. SPECTRUM performs a routine magnetic field scan while collecting the real output of the lock-in. The spectrum is scanned between B_{oMin} and B_{oMax} . FIELD CYCLE performs cycled LFEPR where B_0 is scanned between B_{oMin} and B_{oMax} multiple times while recording the EPR signal. The program records the LFEPR signal while scanning from B_{oMin} to B_{oMax} and back to B_{oMin} multiple times. This type of acquisition is useful for examining a sample for ferro/ferrimagnetism. TIME DOMAIN keeps the B_0 constant while recording the EPR signal. This program is used to determine the signal variation while changing some parameter with respect to time. The shortest time between points is 0.05 second. For example, recording the spatial distribution of the EPR signal containing material when the probe position is varied with respect to time.²⁴ Other programs assist with instrument tuning, such as LOCK-IN PHASE for optimizing the lock-in amplifier phase setting and TUNE for matching v to the resonance frequency of the probe.

2.6 | General operation

The following operational comments are added to help those building a LFEPR. Before a spectrum can be recorded, a standard sample such as a small amount of DPPH is placed in the probe, the probe is matched to 50 Ω , and ν is set to the resonance frequency of the probe. With the 180° hybrid tee, 50 Ω is indicated by zero signal on the output. The phase shifter on the reference arm is set so that an absorption signal is recorded. Unless $L_{\rm S}$ and $L_{\rm R}$ are of equal lengths, $L_{\rm \varphi}$ will have a length set by Equation 2 and determined iteratively until first derivative signal from DPPH is symmetric. The phase of the lock-in signal is adjusted next by varying the phase value until a maximum first derivative signal is obtained. It is often easier to adjust for zero signal and shift the phase by plus or minus 90° to get the maximum.

The linearity of the field sweep is checked with a Hall effect Gauss meter (5180; FW Bell, Acton, MA, USA) by plotting B_0 vs V_C . Our B_0 vs V_C calibration curve had a slope of 18.686 mT/V, an $R^2 = 0.999978$, and a standard deviation of 0.024 mT, less than half the Earth's magnetic field of 0.05 mT. The exact slope of the calibration is determined from the v and g of DPPH. Based on the uncertainty in the

TABLE 2 Maximum modulation amplitude (mT)

	Modulation Frequency	
Modulation Configuration	10 kHz	20 kHz
Saddle coil on single turn solenoid	0.65	0.34
Solenoid coil	2.20	2.00
Helmholtz coil	0.22	0.24

 B_0 of 24 μ T and ν of 1 Hz, a g factor can be determined with an uncertainty of 0.005.

The modulation amplitude ($B_{\rm Mod}$) in mT for each of the three modulation coil configurations was calibrated from a plot of the measured peak-to-peak linewidth ($\Gamma_{\rm PP}$) of a DPPH sample as a function of modulation setting. The maximum modulation amplitude value at 10 and 20 kHz is listed in Table 2 for the saddle, solenoid, and Helmholtz coils.

Perhaps the most challenging aspect of wide-line LFEPR is the small S_{PP} and signal-to-noise ratio (SNR) due to the large Γ_{PP} . The larger Γ_{PP} allows the use of larger B_{Mod} values which can compensate somewhat for the lower SNR. Prudent choice of other acquisition parameters, such as the B_0 sweep rate and the lock-in time constant, will also facilitate optimal SNR. After B_0 has been stepped to a new value, the EPR signal should be allowed to reach an equilibrium value before being sampled. The spin-lattice relaxation time (T_1) and the lock-in time constant (RC) govern the speed at which the signal reaches equilibrium. Most electron T_1 values are <1 μ s and not a factor when compared to RC values of greater than a ms. In the time domain, the RC value determines how quickly the output of a device responds when the input changes either from a signal or noise. RC is the time it takes for the difference between the input and output to change by a factor of e. In the frequency domain, the RC value determines the cut-off frequency ($f_C = 1/_{RC}$) at which attenuation starts. A simple RC filter has an attenuation of -6 dB/Octave (20 dB/Decade) of frequency above f_C . Many lock-in amplifiers are now digital and can implement RC time constants with roll-off rates that are -24 dB/Octave. The reader is directed to this reference for additional information on RC time constants.²⁵

Because the RC time constant changes the response time, an EPR absorption will be distorted if an improper RC and sweep speed combination are chosen. Choosing $t_{\rm Wait} > 5 {\rm RC}$ assures 99% of the possible signal, but is impractical. Choose instead a practical $t_{\rm Wait} > {\rm RC}$ that minimizes undesirable noise in the spectrum. It should be noted that sweeping $B_{\rm o}$ too quickly can also distort an EPR absorption signal irrespective of a short enough time constant value, but this is not a significant problem in wide line EPR.

1.5 1.0 0.5 EPR signal (μV) 0.0 Han blue -0.5 -1.0 Egyptian blue -1.5 Ultramarine blue -2.0 5 10 15 20 $B_o(mT)$

FIGURE 3 Low frequency electron paramagnetic resonance spectra of the three blue pigments ultramarine blue, Han blue, and Egyptian blue recorded with the single turn solenoid probe. Egyptian blue and Han blue spectra are presented $\times 2$ with a three point square convolution smoothing.



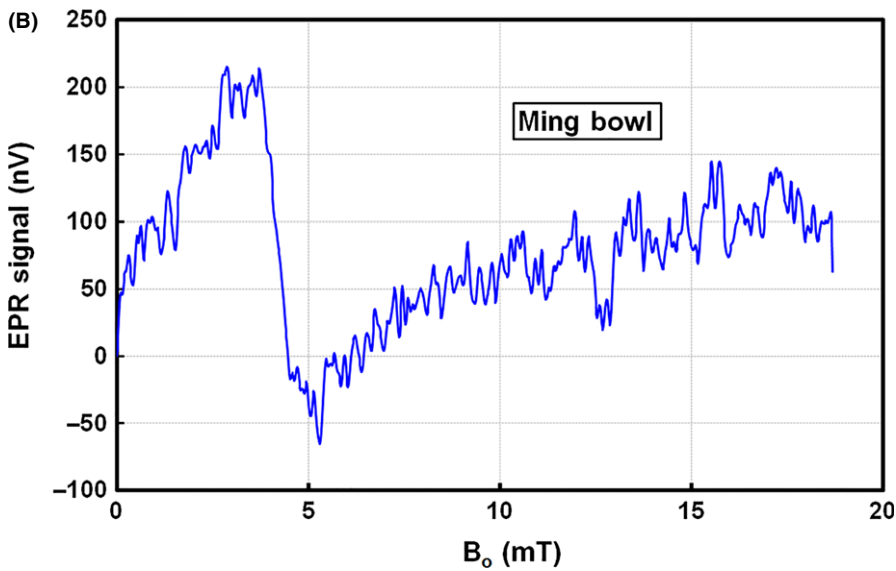


FIGURE 4 Image (A) of a 15.3 cm diameter Ming dynasty bowl in the Helmholtz modulation coil with 2 cm surface coil probe and corresponding low frequency electron paramagnetic resonance spectrum (B).

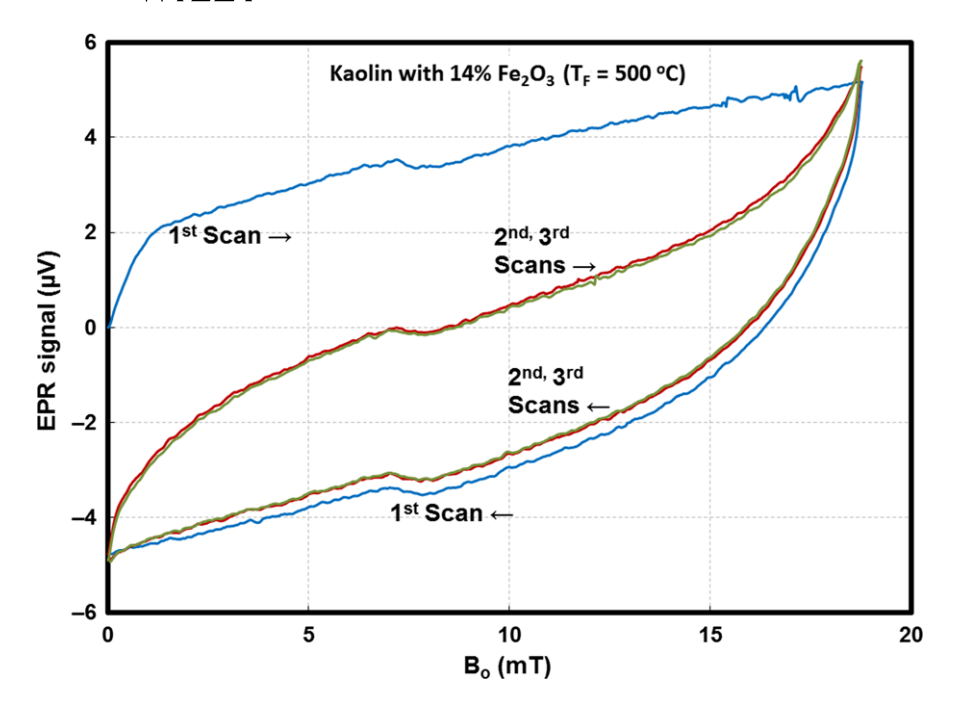


FIGURE 5 Field cycled low frequency electron paramagnetic resonance spectrum of a kaolin clay sample with 14% added Fe₂O₃ showing the effect of ferromagnetism on the spectrum. The first scan with $dB_o/dt > 0$ and then $dB_o/dt < 0$ are unique, while subsequent scans overlap. Only the first two overlapping scans are shown. See text for details

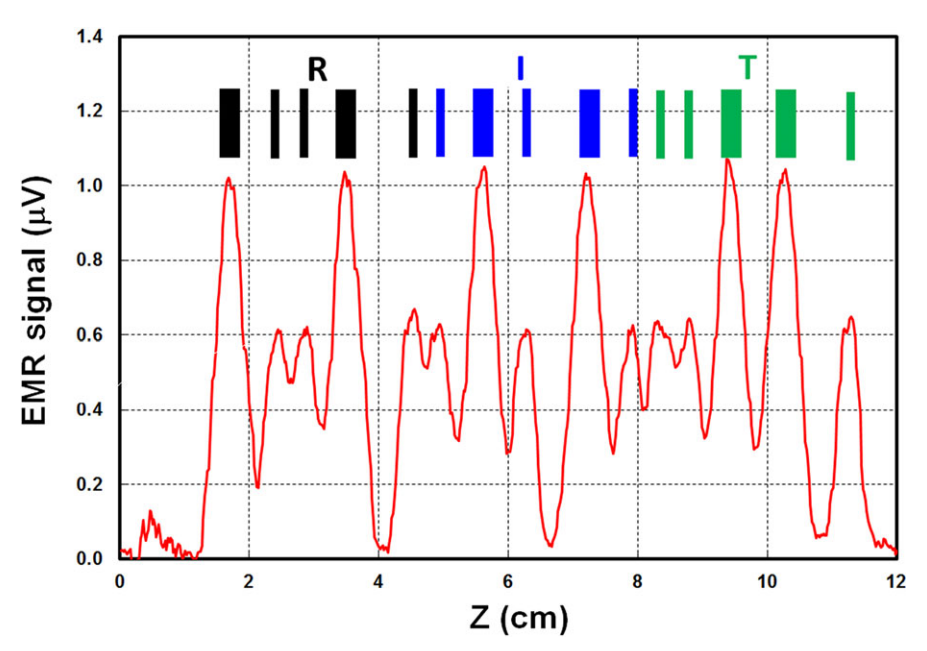


FIGURE 6 Electron paramagnetic resonance signal as a function of the location along the barcode 39 letters RIT printed on paper with electrophotographic toner

3 | TYPICAL SPECTRA

As a demonstration of the capability of the LFEPR spectrometer, we present spectra recorded with three different probes, modulation coils, and LabView acquisition programs.

Figure 3 displays the LFEPR spectra of three common blue pigments: ultramarine (Natural Pigments, Willits, CA, USA), Egyptian blue (Kremer Pigments, New York, NY, USA), Han blue (Kremer Pigments). Spectra were recorded using the STS coil at, respectively, $\nu = 298.848$, 298.780, and 298.819 MHz; 2000 points; $B_{\text{Mod}} = 0.09 \text{ mT}$;

RC = 0.1 second; and LabView program SPECTRUM. Ultramarine (Na₈₋₁₀A₁₆Si₆O₂₄S₂₋₄) possesses an EPR signal from an S_3^- radical ion with a g=2.029-2.030. 26,27 Egyptian blue (CaCuSi₄O₁₀) has an EPR signal from the paramagnetic Cu(II) with anisotropic g factors $g_{//}=2.32$ -2.34 and $g_{\perp}=2.055$ -2.060. 4,28 Han blue (BaCuSi₄O₁₀) is similar to Egyptian blue except that Barium is substituted for Calcium in the lattice. The anisotropic g factors are $g_{//}=2.342$ and $g_{\perp}=2.063$. 29 The Γ_{PP} values in the LFEPR signals from the three pigments differ and are 2.3, 10.5, and 3.5 mT, respectively. Evidence of an anisotropic g factor is difficult to discern in the spectra. This figure

shows one challenge with LFEPR, specifically, determining the baseline when very broad lines are observed. The best way to set the baseline is to scan to a high enough B_0 that the shoulders of the peak have reached zero.

Figure 4A is an image of a Ming Dynasty porcelain bowl in the Helmholtz modulation coil with the 2-cm surface coil on the bottom the bowl. The bowl is made of kaolinite and has Fe (III) impurities in the lattice giving a very small g=4 signal shown in Figure 4B. The LabView program SPECTRUM was used to record the 1000 point spectrum at v=245.70 MHz with RC = 0.3 second, 3 averages, $B_{\rm Mod}=0.16$ mT, and a 7 point triangular convolution.

A 1.2 cm diameter, 7 cm long, rod-shaped sample of EPK kaolin clay (Edgar Minerals, Hawthorne, Fl, USA) with 14% added Fe₂O₃ (Sigma-Aldrich, St. Louis, MO, USA) was fired at 500°C for 24 hours. Its LFEPR spectrum was determined with the 440 MHz STS resonator. The sample was determined to be ferro/ferrimagnetic using LabView program FIELD CYCLE shown in Figure 5. The spectra contain a large initial increase in signal before 1.5 mT, then a more gradual rise to the end of the scan, both attributed to the ferro/ferrimagnetism; and a small g = 4 paramagnetic resonance peak. The first upfield and downfield scans are unique as the sample is retaining magnetization. Subsequent scans overlap with each other as the ferromagnetic domains retain some alignment from exposure to the 18 mT magnetic field.

The utility of the LabView program TIME DOMAIN is presented in Figure 6. The barcode 39 version of the letters RIT were electrophotographically printed on a piece of 75 g/m² weight, 92 bright, white recycled copy paper (620016; Staples, Framingham, MA, USA) with an electrophotographic printer (LaserJet 1200; Hewlett-Packard, Palo Alto, CA USA) using toner (OfficeMax, Boca Raton, FL, USA) formulated for this HP printer. Laser printer toner is known to have ferromagnetic particles to help the magnetic brushes of the print engine control the toner.³⁰ The particles have a broad 150 mT EMR signal at 9 GHz.³¹ For printed toner on paper, it is only possible to discern a gradual increase in signal over the 18 mT scan range of the LFEPR.²⁴ Instead of fixing B_0 at the spectral peak, the magnetic field was set at 7.5 mT and the barcode moved under the probe to yield the spectrum of Figure 6. The higher signal peaks correspond to the broader bars and the lower peaks the narrower bars in the code.

4 | CONCLUSIONS

A design for a low frequency EPR spectrometer suitable for wide-line spectroscopy between 100 and 500 MHz was

presented. The components for the spectrometer are readily available commercially. The spectrometer is suitable for non-destructively and non-invasively studying the EPR signals from paramagnetic metal ions or stable radicals in the pigments of paint, paramagnetic and ferromagnetic properties of ceramics, and Mn(II) in marble. The magnet of the spectrometer can accommodate 15 cm diameter objects which are meters in length. Objects up to 30 cm in diameter may be studied by incorporating a larger diameter modulation coil.

ACKNOWLEDGMENTS

MH and BEB acknowledge support from the NSF Physics Directorate REU program "Imaging in the Physical Sciences" under award number 1359361.

ORCID

Joseph P. Hornak http://orcid.org/0000-0003-1016-9849

REFERENCES

- Poole CP. Spin Resonance, 2nd edn. New York: John Wiley & Sons; 1983:780.
- Pierik AJ, Hagen WR. S=9/2 EPR signals are evidence against coupling between the siroheme and the Fe/S cluster prosthetic groups in Desugovibrio vulgaris (Hildenborough) dissimilatory sulfite reductase. Eur J Biochem. 1991;195:505-516.
- Quinet P, Biémont E. Lande g-factors for experimentally determined energy levels in doubly ionized lanthanides. At Data Nucl Data Tables. 2004;87:207-230.
- Orsega EF, Agnoli F, Mazzocchin GA. An EPR study on ancient and newly synthesised Egyptian blue. *Talenta*. 2006;68:831-835.
- Moretto LM, Orsega EF, Mazzocchin GA. Spectroscopic methods for the analysis of celadonite and glauconite in Roman green wall paintings. J Cult Herit. 2011;12:384-391.
- Mazzocchin GA, Agnoli F, Salvadori M. Analysis of Roman age wall paintings found in Pordenone, Trieste and Montegrotto. *Talanta*. 2004;64:732-741.
- Gobeltz N, Demortier A, Lelieur JP, Duhayon C. Correlation between EPR, Raman and colorimetric characteristics of the blue ultramarine pigments. *J Chem Soc, Faraday Trans*. 1998;94:677-681.
- 8. Raulin K, Gobeltz N, Vezin H, Touati N. Led, Identification of the EPR signal of S2⁻ in green ultramarine pigments. *Phys Chem Chem Phys.* 2011;13:9253-9259.
- Dietemann P. Towards More Stable Natural Resin Varnishes for Paintings. The Aging of Triterpenoid Resins and Varnishes. Zurich: Federal Institute of Technology; 2003.
- Christiansen MB, Sørensen MA, Sanyova J, Bendix J, Simonsen KP. Characterisation of the rare cadmium chromate pigment in a 19th century tube colour by Raman, FTIR, X-ray and EPR. Spectrochim Acta Part A Mol Biomol Spectrosc. 2017;175:208-214.
- Sales KD, Oduwole AD, Convert J, Robins GV. Identification of jet and related black materials with EPR spectroscopy. *Archaeometry*. 1987;29:103-109.

- Marinescu M, Emandi A, Duliu OG, Stanculescu I, Bercu V, Emandi I. FT-IR, EPR and SEM-EDAX investigation of some accelerated aged painting binders. Vib Spectrosc. 2014;73:37-44.
- Lakshmi Reddy S, Reddy G, Ravindra Reddy T, et al. XRD, TEM, EPR, IR and nonlinear optical studies of yellow ochre. J Laser Opt Photonics. 2015;2:120.
- Polikreti K, Maniatis Y. A new method for the provenance of marble based on EPR spectroscopy. Archaeometry. 2002;44:1-21.
- Polikreti K, Maniatis Y. Distribution of changes of Mn(II) and Fe (III) on weathered marble surfaces measured by EPR spectroscopy. Atmos Environ. 2004;2004:38.
- Cordischi D, Monna D, Segre AL. ESR analysis of marble samples from Mediterranean quarries of archaeological interest. *Archaeometry*. 1983;25:68-76.
- Maniatis Y. Scientific techniques and methodologies for the provenance of white marbles. In: Martini M, Milazzo M, Piacentini M, eds. *Proceedings of the International School of Physics Enrico Fermi*. Amsterdam: IOS; 2003: 179-202.
- Maniatis Y, Tambakopoulos D, Dotsika E, Stefanidou-Tiveriou T. Marble provenance investigation of Roman sarcophagi from Thessaloniki. *Archaeometry*. 2010;52:45-58.
- Hornak JP, Spacher M, Bryant RG. A modular low frequency ESR spectrometer. *Meas Sci Technol*. 1991;2:520-522.
- Wertz JE, Bolton JR. Electron Spin Resonance. London: Chapman and Hall; 1986:497.
- Eaton GR, Eaton SS, Barr DP, Weber RT. Quantitative EPR. New York: Springer Wein; 2010:185.
- 22. Szczepaniak E, Hornak JP. ESR imaging based on the modulation-field phase. *J Magn Reson*, Ser A. 1993;104:315-320.
- Hornak JP, Szumowski J, Bryant RG. Elementary single turn solenoids used as the transmitter and receiver in magnetic resonance imaging. *Magn Reson Imaging*. 1987;5:233-237.

- Switala LE, Ryan WJ, Hoffman M, Brown W, Hornak JP. Low frequency EPR and EMR point spectroscopy and imaging of a surface. *Magn Reson Imaging*. 2016;34:469-472.
- 25. Stanford-research-systems. About lock-in amplifiers; 2017:1-9.
- Wieckowski A. Ultramarine study by EPR. *Physica Status Solidi* (B). 1970;42:125-130.
- Eaton GR, Eaton SA, Stoner JW, et al. Multifrequency electron paramagnetic resonance of ultramarine blue. *Appl Magn Reson*. 2001;21:563-570.
- Mirti P, Appolonia L, Casoli A, et al. Spectrochemical and structural studies on a Roman sample of Egyptian blue. Spectrochim Acta. 1995;51A:437-446.
- Chuanyi L. Electronic structures of square planar coordinated transition metal ions in compounds with gillespite structure. *Chin J Geochem.* 1990;9:132.
- Hauser OG. Electrophotography. In: Hornak JP, ed. *Encyclopedia of Imaging Science and Technology*, Vol. 1. New York: John Wiley & Sons; 2002:299-331.
- Lobanov NN, Nikiforov VN, Gudoshnikov SA, et al. Differentiation of magnetic composites in terms of their nanostructural organization. *Dokl Chem.* 2009;426:96-100.

How to cite this article: Switala LE, Ryan WJ, Hoffman M, Javier S, Black BE, Hornak JP. A wideline low frequency electron paramagnetic resonance spectrometer. *Concepts Magn Reson Part B*. 2017; e21355. https://doi.org/10.1002/cmr.b.21355